Journal of Polymers and the Environment (2023) 31:2705–2714
https://doi.org/10.1007/s10924-022-02693-x

ORIGINAL PAPER

Physico-chemical Characteristics of Biodegradable Poly(lactic acid) and Poly(lactic acid)/Chitosan Nano-Composites Under the Influence of Gamma Irradiation

Moataz A. Elsawy[1] · Mohamed Fekry[1] · Aisha M. Sayed[2] · Nabila A. Maziad[3] · Gamal R. Saad[2]

Accepted: 15 November 2022 / Published online: 23 January 2023

Abstract
PLA and its nanocomposite containing 3% chitosan nanoparticles (PLA-3CsNP) were studied to see how γ -irradiation affected their characteristics. Different doses of γ -irradiation were applied to the investigated materials under inquiry (5–40 kGy) using ^{60}Co at ambient conditions. The irradiation materials were characterized by FT-IR, GPC, mechanical tensile test, DSC, XRD, and TGA in solid and chloroform solutions. The molecular weight of the studied materials was lowered when the irradiation dose was increased, indicating that γ-irradiation had the dominating effect through oxidative degradation, and chain scission. The addition of chitosan to PLA reduces the impact of γ-irradiation, while the samples irradiated in solution showed more degradation after irradiation than irradiated solid films. Irradiation caused a decrease in tensile strength and elongation at break values. Both the melting temperature (Tm) and the glass transition temperature (Tg) decreased as the irradiation dose was increased. The crystallization peak temperatures were reduced when pure PLA was irradiated in solution. The thermal stability of PLA was diminished as the irradiation dose was raised, and this effect was more pronounced in samples irradiated in chloroform solution.

Keywords γ-Irradiation · PLA · PLA/chitosan nanoparticles composite · Mechanical properties · Thermal properties

Introduction

In recent decades, it has been a rise in environmental consciousness. As a result, biopolymers such as polylactic acid (PLA) have increased in various applications. PLA is the most crucial option to replace petroleum-based polymers such as plastic waste in multiple industries, including transportation, electrical, and electronic sectors, due to its good physical and mechanical qualities, reasonable cost, and processing with traditional techniques. PLA can be considered attractive, sustainable, eco-friendly, degradable, and recyclable [1, 2]. The polymerization of lactic acid obtained from the fermentation of various naturally accessible polysaccharides such as potato, sugarcane, corn, and starch produces PLA, a linear aliphatic thermoplastic polyester. Biodegradability, biocompatibility, thermal flexibility, high dyeability, and nontoxicity are just a few characteristics that make it ideal for biomedical, flame retardant, food packaging, and agricultural applications [3–6]. However, the drawbacks of PLA including its brittleness, thermal stability and low crystallization rate restrict its uses, especially for structural applications. These drawbacks can be avoided and tailor-modified to specific applications by several methods such as blending of PLA with other polymers [7, 8], copolymerization with synthetic [9, 10] and cyclic monomers like glycolide, ε-caprolactone, γ-valerolactone, trimethylene carbonate, etc. as well as linear monomers like ethylene glycol [11] or crosslinking [12, 13].

On the other hand, PLA has flaws such as low toughness, brittleness, and heat resistance. Composites and

✉ Moataz A. Elsawy
mo3taz_elsawy@yahoo.com; moataz@epri.sci.eg

✉ Gamal R. Saad
grsaad@sci.cu.edu.eg

[1] Polymer Laboratory, Petrochemical Department, Egyptian Petroleum Research Institute, Nasser City, Cairo 11727, Egypt

[2] Department of Chemistry, Faculty of Science, Cairo University, Cairo 12613, Egypt

[3] Polymer Chemistry Department—National Center for Radiation Research and Technology, Atomic Energy Authority, Nasr City, Egypt

nanocomposites must be prepared by adding stiff fillers as reinforcement materials [14, 15].

Recently, PLA has been combined with natural nanoparticles formed from polysaccharides, such as rod-like whickers of chitin and cellulose and platelet-like nanocrystals of starch, to obtain entirely renewable mechanical characteristics, low processing costs, and biodegradable nanocomposites. Therefore, PLA is re-engineered to improve its thermal, rheological, barrier and mechanical properties through nanoparticles (NPs) reinforcement [16].

However, the hydrophilic nanoparticle granules and the hydrophobic PLA have a weak interfacial contact. To overcome these restrictions, researchers looked into modifying, processing, and the qualities of mixes to improve phase compatibility [17, 18]. These particles have some of the benefits of natural polymers and some of the general properties of nanomaterials, such as tiny size, surface, and interface effects. Chitosan (CS) is a polysaccharide of D-glucosamine derived from chitin with antibacterial, antifungal, mucoadhesive, and hemostatic properties. CS has consequential applications in pharmaceutical, biomedical, chemical, agricultural, environmental, material science, food industries, delivery, coating applications, hydrogels, membranes, beads, porous foams, nanoparticles, microparticles, sponges, and nanofibers/scaffolds [19], [20]. The incorporation of chitosan nanoparticles into the PLA matrix led to improved mechanical behavior and crystallization rate of PLA. The application of PLA and its composites in biomedical and food packaging applications make it necessary for complete sterilization of the products. The main sterilization process of polymers for medical applications is by γ-radiation [21, 22]. However, irradiation may affect the stability of the product and thus its safety of use. Irradiation exposure has a substantial impact on the degrading characteristics of polymer matrices. As a result, it's critical to look at the chemical and physical effects of energy transfer on polymer matrices [23]. The effects of γ-radiation on PLA, PLA blends, and various PLA nanocomposite were investigated. As a result of chain scissions, γ-irradiation can lower the molecular weights of polymers. Higher doses can cause polymer cross linking. The chain scission effect is the most prominent in PLA [24–27]. In our previous work [21], they reported that incorporation of 3.0% content of CsNP is the most effective and economical method to attain desired mechanical and thermal properties without meddling with the inherent benefits in the neat PLA matrix.

Based on the above findings, the goal of this study is to see how γ -irradiation affects the mechanical and thermal properties of pure PLA and PLA composites with 3% CsNP; *namely PLA-3CsNP*. Film and solution samples in chloroform, as the solvent, are irradiated at dosage intervals ranging from 0 to 40 kGy. The molecular structure, molecular weight, mechanical tensile properties, and thermal properties of pure PLA and its composite were evaluated as a function of irradiation dose.

Experimental

Materials

Nature Works® LLC (Minnetonka, USA) provided the polylactic acid (PLA) (IngeoTM3001D), which was dried at 100 °C for 3 h before usage. G.T.C Bio Corporation provided chitosan nanoparticles CsNP (CN001) (deacetylated 96%) with particle sizes ranging from 150 to 280 nm (Hongkong, China). The chitosan nanoparticles were dried in a vacuum oven at 80 °C for 24 h. Chloroform ($CHCl_3$) (99.8% purity) was obtained from sigma Aldrich (USA).

Sample Preparation

A twin screw extrusion melting manufacturing technique was used to create both neat PLA and PLA composites incorporating 3wt% chitosan nanoparticles (CsNP), Thermo Scientific provided the Prism Eurolab 16 co-rotating twin-screw extruder, which used to prepare the samples. The screw configuration was strong, with three mixing zones that included mixing discs positioned at 90 degrees. For two hours, the mixing temperature was 180 °C [21]. To obtain sheets of 0.2 mm thickness, the prepared samples were hot pressed for 5 min at 185 ± 2 °C and 10 MPa, respectively, and then cooled pressed at room temperature for another 5 min. Before any testing, the moulded sheets were stored for 48 h at room temperature.

Gamma Irradiation Exposure Test

Through the Center for Radiation Research and Technology (NCRRT) in Cairo, Egypt exposed neat PLA and PLA nanocomposite sheets (20 × 20 cm) to gamma radiation using ^{60}Co industrial equipment (manufactured in Russia). At ambient temperature in the presence of air, the samples were exposed to irradiation doses of 0, 5, 10, 15, 20, 25, 30, 35, and 40 kGy with a dose rate 4.774 kGy h^{-1}. PLA and PLA-3CsNP composite loaded with 3% CsNP were both irradiated in $CHCl_3$ solution under the same circumstances. The PLA and its nanocomposites concentration in solution were prepared as 1.0 g/ 50 mL chloroform. For PLA nanocomposites, the mixture was sonicated for 2.0 h before subjected to the irradiation. The PLA and its nanocomposite in $CHCl_3$ solution were then placed onto a glass dish after being irradiated. After the chloroform solvent had evaporated after 24 h at room temperature, thin solid films (f) of 0.1–0.12 mm thickness were produced, they denote as PLA-f and PLA-3CsNP-f.

Measurements

Fourier-Transform Infrared (FT-IR) Spectroscopy

FTIR spectra over the range 500–4000 cm^{-1} were performed by FTIR spectrophotometer type Mattson 100 Unicam, England. A dry constant weight from each sample was ground with 30 mg of KBr and then pressed to form discs. Before measurements, the samples for FT-IR analysis were first dried in a vacuum oven for 2 h at 80 °C.

Gel Permeation Chromatography (GPC)

The average molecular weights ($\overline{M}_w$ and $\overline{M}_n$) of PLA samples and its nanocomposites in tetrahydrofuran (THF) as solvent were determined by Waters Model 515/2410 using a gel Permeation Chromatographic technique (GPC, Waters, America). PLA samples and its nanocomposites were previously dissolved for 24 h in THF (5 mg/ml) under stirring. The filtration of solutions was tested through 0.45 mm stainless steel frits prior to injection. THF was used as eluent using 1 mL/min as a flow rate at room temperature.

Gel Fraction Test

Soxhlet extraction with chloroform as the solvent was used to determine the gel content. After a 24-h extraction process, the insoluble fraction was dried for 48 h in a vacuum oven and weighed. Using the following Eq. (1), the quantity of gel (cross-linked) fraction was determined gravimetrically

$$\text{Gelfraction}(\%) = \frac{W_2}{W_1} \times 100 \tag{1}$$

where, w_1 and w_2 represent the samples' weights before and after extraction, respectively. Three determinations were used to get the average values.

Mechanical Analysis

An Instron universal tester (1191) (US) with a crosshead speed of 20 mm/min and a load cell of 1000 N was used to perform mechanical tests such as tensile strength and elongation at break. The specimen sheets were cut into dumbbell shapes with thicknesses ranging from 0.10 to 0.12 mm and tested at room temperature for tensile strength and elongation at break according to ASTM D 638 requirements.

X-Ray Diffraction (XRD)

A Shimadzu XRD-6000 series (China) apparatus with a Ni-filter and a Cu-K target that generates a voltage of 30 kV and a current of 20 mA from a Cu–K radiation source (= 1.54056 A) was used to obtain the XRD patterns of unirradiated and irradiated PLA and its nanocomposite. The X-ray diffractograms were taken in the angle range of 2 to 50° at a scan rate of 2 °C/min.

Thermal Analysis

A TA instruments (USA) Q20 differential scanning calorimeter was used to perform DSC measurements under nitrogen purge (30 mL/min). Indium and lead melting temperatures and enthalpies were utilized to calibrate the instrument. About 3–5 mg of the polymer was placed in an aluminium pan for sampling. Each sample was heated from 25 to 190 °C at a rate of 10 °C/min, then cooled at the same rate to 25 °C. The second heating run curve yielded the glass transition temperature (T_g), melting enthalpy (ΔH_m), melting temperature (T_m), crystalline temperature (T_c), and crystalline enthalpy (ΔH_{cc}). The T_g was measured halfway through the specific heat capacity increment. The peak values of the corresponding exothermal and endothermal processes in the DSC thermograms were T_c and T_m. From the melting enthalpy, we can obtain the degree of crystallinity X_c in the sample by this Eq. (2):

$$\text{Xc}\% = \frac{1}{W_{PLA}}\left(\frac{\Delta H_m}{\Delta H_m^0}\right) \times 100 \tag{2}$$

where ΔH_m^0 is the melting enthalpy of a 100 percent crystalline PLA sample (= 93 J g^{-1}) [28] and w_{PLA} is the weight fraction of PLA in the sample.

Thermogravimetric analysis (TGA) was performed by a Shimadzu-30 (TGA-30) (China). The samples were heated from 25 to 600 °C at a rate of 10 °C min^{-1} in a nitrogen environment at 50 mL/min. For all of the trials, the sample weights were between 3 and 5 mg.

Results and Discussion

FTIR

The ability of gamma radiation to produce structural changes in PLA and PLA/3CsNP composite was investigated using FTIR analysis. Figure 1 displays FTIR data in 4000–400 cm^{-1} for both non-irradiated and irradiated PLA. Strong symmetric and asymmetric CH stretching modes in the CH_3 and C-H groups are responsible for the peaks at 3010 and 2911 cm^{-1}, respectively. The intensity of the two peaks increases as the radiation dose increases. The peak at 1445 cm^{-1} corresponds to the bending vibration of CH_3 and C-H groups [29, 30]. Also, the intensity of this peak appears to rise as the radiation dose is increased. The spectra

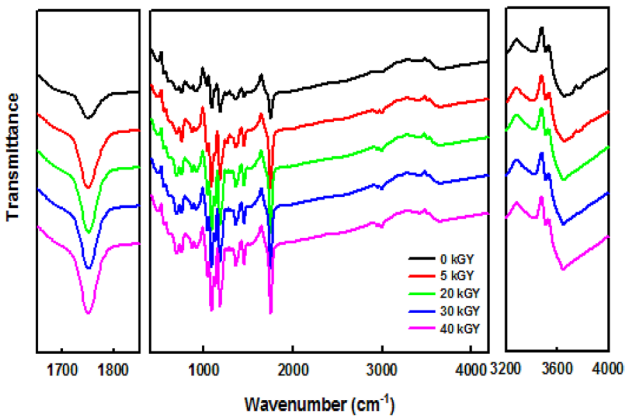

Fig. 1 FTIR spectra of γ-irradiated PLA at different doses in chloroform

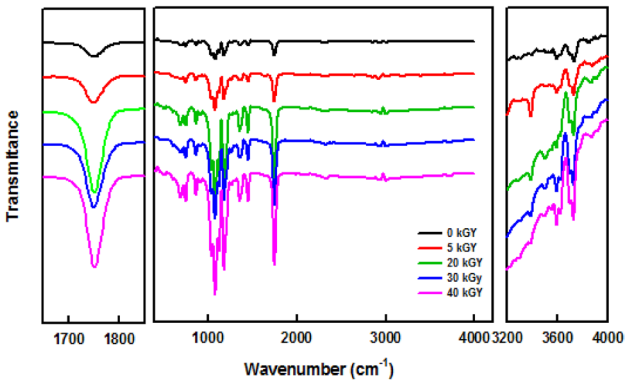

Fig. 2 FTIR spectra of γ-irradiated PLA-3CsNP composite at different doses in chloroform

show main characteristic peaks of PLA at 1752, 1180 and 1085 cm^{-1}corresponding to C = O stretch, C–O–C antisymmetric stretch and C–O–C symmetric stretch of ester linkage, respectively. No pronounced changes are observed in the chemical structure of the irradiated samples (5, 20, 30, and 40 KGy) compared to that of non-irradiated one (0 KGy). Only slight increases occurred at the intensity at the same wavenumber with increase the radiation dose. The band corresponding to the C=O at 1752 cm^{-1} (Yıldırım &Oral 2018) which intensifies and slightly shifts to higher wavenumber with increasing the γ-irradiation dose.

Figure 2 shows FTIR data of non-irradiated and irradiated PLA-3CsNP. Most of the chitosan signature peaks following irradiation indicate that gamma irradiation did not cause their associated structural modes to deteriorate. There are few discrepancies in the FTIR spectra of irradiated and non-irradiated substances. Irradiation causes an increase in the intensity of peaks at 3400 cm^{-1}, which is due to the hydroxyl groups. These changes in absorption peaks could be attributed to the PLA's polymeric chains scission mechanism and the subsequent oxidation reactions induced by the γ-irradiation [24]. In the region of 500–600 cm^{-1}, a band of multiple peaks resulting from oxidative deterioration due to gamma irradiation occurs. CO stretching and OH bending are thought to be responsible for this band [31]. Another peak appeared around 1750 cm^{-1} after irradiation, and its intensity increased as the radiation dose increased.

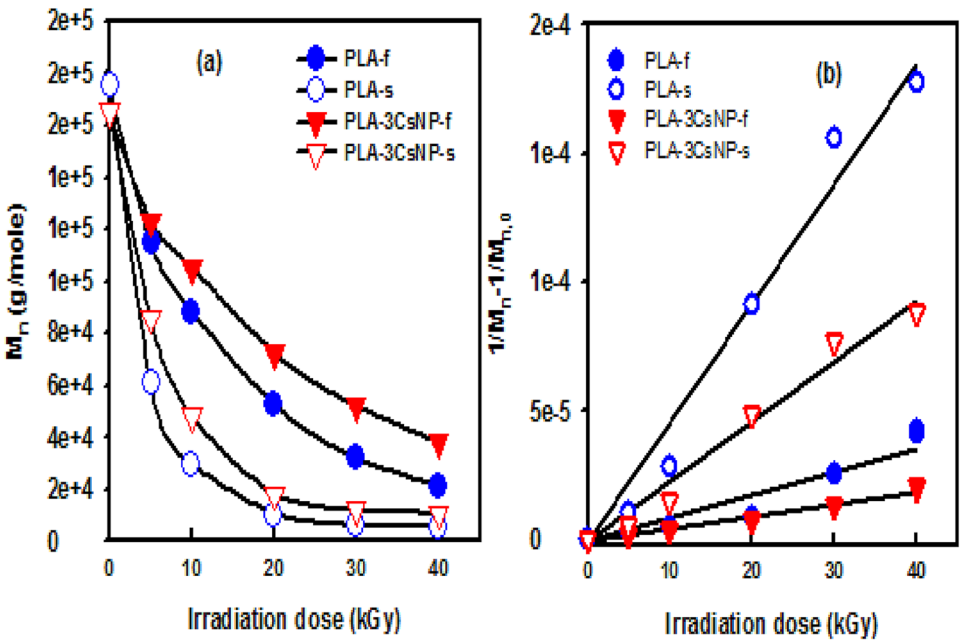

Fig. 3 Plots of **a** the number average molecular weight ($\overline{M}_n$) and **b** $1/\overline{M}_n - 1/\overline{M}_{n,0}$ as a function of irradiation doses of PLA and PLA composite in solid film and solution in chloroform

Molecular Weight Change

In the absence and presence of CsNP filler, Fig. 3a demonstrates the effect of irradiation dose on the number-average molecular weight ($\overline{M}_n$) of the PLA. As indicated, the reduction of $\overline{M}_n$ in chloroform-irradiated samples is more significant than that of irradiated films. The addition of filler has a less apparent effect on $\overline{M}_n$ reduction. Depending on the irradiation circumstances, gamma-irradiation causes free radical sites on the PLA backbone by abstracting hydrogen from PLA, resulting in chain scission or development of branched/cross-linked structures. Thus, the decrease in $\overline{M}_n$ indicates that chain scissions of PLA's main backbone are predominantly under the influence of ionizing γ-radiation action. Irradiation can also cause cross-linking reactions, especially at higher dosages [12]. Gel tests were done on the irradiation samples to confirm that such reactions had occurred. The gel content in the PLA and PLA-3CsNP samples treated to 40 kGy radiation in chloroform is roughly 3.8 ± 0.7 and 2.1 ± 0.5%, respectively. Because the tested interval doses were below gel dosage, the gel content for the remaining exposure doses is either too low to be considered or equal to zero. These findings are in line with previous studies [32, 33]. The radiation chemical yield of degradation (scission) Gs is calculated using the Alexander–Charlesby–Ross Eq. (3) assuming chain scission is the only action mode of radiation [34].

$$\frac{1}{\overline{M}_n} = \frac{1}{\overline{M}_{n,0}} + 1.04 \times 10^{-7} G_S \times D \tag{3}$$

where $\overline{M}_{n,0}$ and $\overline{M}_n$ represent the number average molecular weights of initial and final PLA at an absorbed dose (D), respectively.

The plot of $(1/\overline{M}_n - 1/\overline{M}_{n,0})$ against irradiation dose of the PLA and PLA-3CsNP composite is shown in Fig. 3b. The satisfactory obtained straight line suggests that degradation scission is random. Degradation scission yield (Gs) is found to be 0.98 and 4.79, for their radiated PLA in solid film (f) and CH_3Cl solution (s), respectively. The Gs values of PLA-3CsNP are 0.48 and 2.34 for samples irradiated in solid and solution state, respectively. This indicates that the samples irradiated in solution are more susceptible to degradation compared with that irradiated in solid upon subjecting to γ-irradiation. The lower Gs values of the polymer composite compared to the neat polymer suggest that the PLA composite degradation upon irradiation is less severe compared with pure PLA [35].

Tensile Properties

The γ-irradiation dose effect on both tensile strength and elongation properties of cast films of neat PLA and its composite is shown in Fig. 4a,b. It shows that adding 3% chitosan to PLA diminishes tensile strength while increasing elongation. With increasing the radiation dose, the tensile strength and elongation of irradiated neat PLA and its composite tested films at break decreased steadily, demonstrating that irradiation makes the material more brittle. According to the results of molecular weight studies, the decrease in mechanical characteristics could be due to a reduction in molecular weight as a result of random PLA polymeric chain scissions that increase with increasing γ-irradiation dose. The mechanical characteristics of irradiated samples in solution could not be examined after irradiation due to their high fragility and destruction.

Differential Scanning Calorimetry

Figures 5, 6, 7, 8 show the DSC curves of neat PLA and PLA-3CsNP irradiated in solid state and cast films from CH_3Cl solution after irradiation. Table 1 summarizes the transition parameters calculated from these curves. A thermogram of the unirradiated neat PLA reveals three thermal

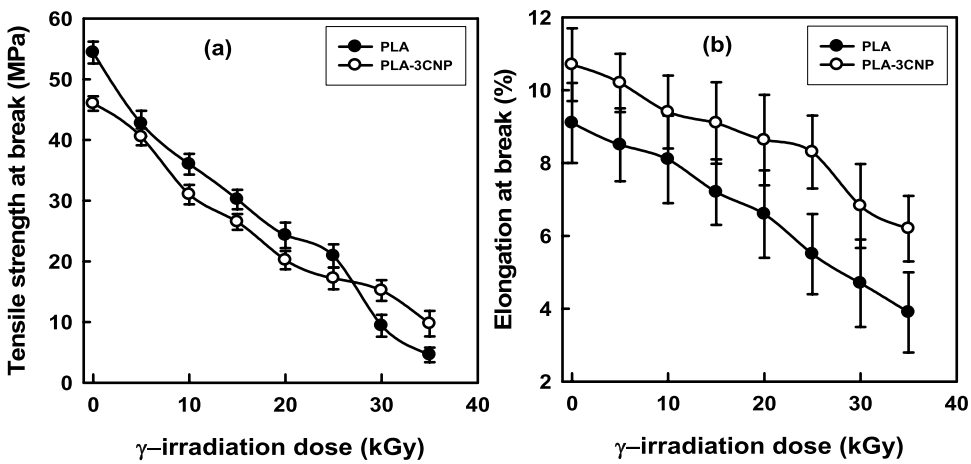

Fig. 4 Plots of the tensile strength (**a**) and elongation % at break (**b**) of PLA and PLA composite irradiated films

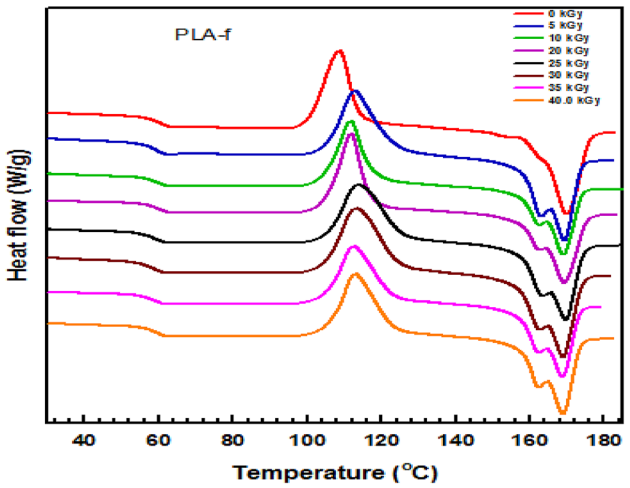

Fig. 5 DSC thermograms of un-irradiated and irradiated PLA films at various γ-irradiation doses

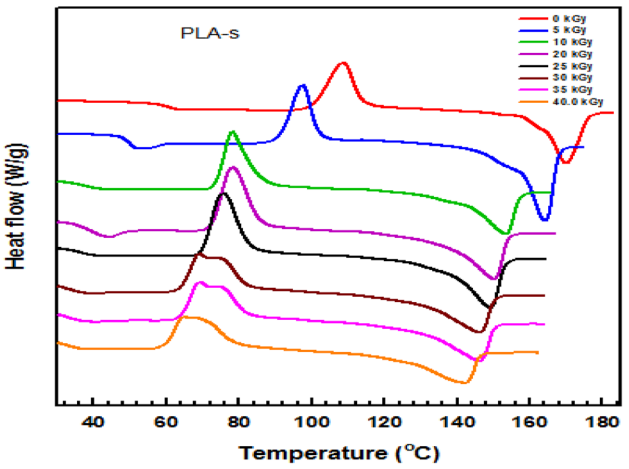

Fig. 7 DSC thermograms of un-irradiated (0 KGy) and irradiated PLA in $CHCl_3$ solution at various γ-irradiation doses

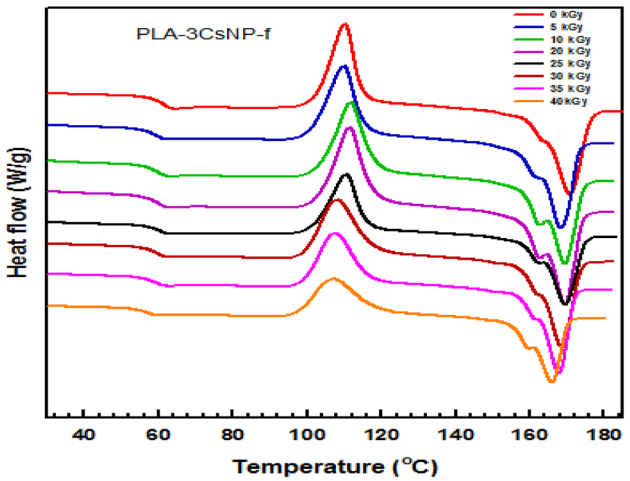

Fig. 6 DSC thermograms of un-irradiated (0 KGy) and irradiated PLA-3CsNP films at various γ-irradiation doses

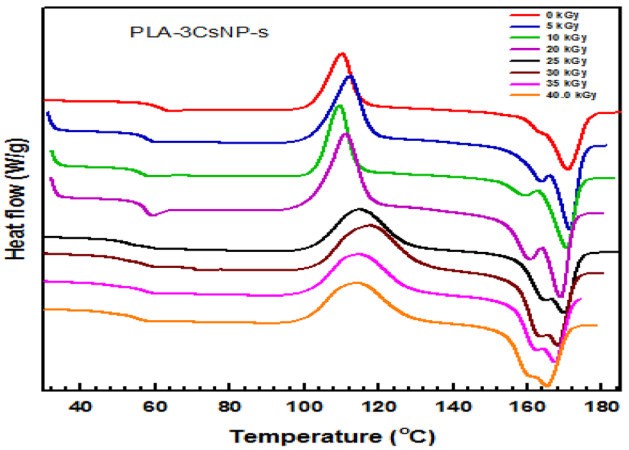

Fig. 8 DSC thermograms of unirradiated (0 KGy) and irradiated PLA-3CsNP in $CHCl_3$ solution at various γ-irradiation doses

transitions at 61.5, 108.7, and 170.4 °C, respectively, corresponding to the glass transition, exothermic peak temperature (T_c), and endothermic melting peak temperature (T_m). The T_g and T_m of irradiated solid samples of neat PLA and PLA-3CsNP drop little when the irradiation dose increases. This could be attributed to the production of PLA chains with reduced molecular weight and a decrease in crystalline shape perfection, crystallite quantity in terms of reduction surfaces beneath melting peaks, and crystallite size distribution narrowing [27, 32, 36]. The imperfections created by irradiation increase chain mobility, causing the amorphous phase to occur at lower temperatures. Irradiated samples also had two melting peaks, indicating that during irradiation, two different types of crystallites and/or differing lamella thicknesses were produced. In terms of the exothermic crystallisation peak exhibited on cooling, no significant changes in its maximum, T_c, are detected after irradiation treatment within the dosage intervals investigated. Table 1 further shows that as the irradiation dose increases, the melting enthalpy and thus the extent of crystallinity drops significantly, indicating that the random main chain scissions caused by irradiation have happened both in the crystalline and amorphous regions of the polymer. Additionally, it is obvious that the decline of the Tg, Tc and Tm parameters become more pronounced for neat PLA after irradiated in CH_3Cl solution and casting, indicating that the degradation process mediated by γ-irradiation in solution is more dramatic than in a solid state. The decrease in these transition parameters confirms that irradiation of PLA in CH_3Cl produces more homogeneous short chains with fewer entanglements than irradiation of PLA in a solid state, enhancing

Table 1 DSC data of PLA and PLA /3CNPs irradiated with γ-irradiation doses

Sample	Dose (kGy)	T_g (°C)	T_c (°C)	T_m (°C)	ΔH_c (J/g)	ΔH_m (J/g)	X_c (%)
PLA-f	0.0	61.5	108.7	170.4	30.3	38.8	41.1
	5.0	60.5	113.5	171.1	33.2	38.2	40.0
	10.0	59.6	112.9	169.4	36.2	37.2	40.8
	20.0	60.1	111.8	169.3	34.0	38.4	41.3
	25.0	59.4	113.8	169.7	28.5	36.0	38.7
	30.0	58.7	113.3	169.0	31.1	37.1	39.9
	35.0	58.8	112.6	168.8	26.9	36.6	39.4
	40.0	56.2	112.9	168.9	33.0	35.1	38.4
PLA-3CsNP-f	0	61.9	110.1	170.8	35.8	38.2	42.3
	5.0	60.2	110.0	168.4	33.7	38.0	42.1
	10.0	59.2	111.7	169.4	32.8	37.1	41.1
	20.0	60.7	110.5	169.6	30.9	36.2	40.1
	25.0	59.8	108.1	168.6	32.2	36.5	40.5
	30.0	59.2	107.5	167.9	32.7	36.0	39.9
	35.0	59.4	109.1	168.0	30.6	36.1	40.1
	40.0	56.8	104.8	167.2	30.0	36.7	40.7
PLA-s	0.0	61.5	108.7	170.4	30.3	38.8	41.3
	5.0	49.9	96.7	164.2	35.8	39.3	42.3
	10.0	40.4	79.7	153.1	32.4	38.3	41.2
	20.0	38.8	78.2	150.0	34.9	38.7	41.6
	25.0	39.1	79.7	151.1	37.0	37.1	39.9
	30.0	33.4	69.6	146.1	30.5	35.3	38.0
	35.0	34.1	68.1	146.0	30.8	34.2	36.8
	40.0	32.4	64.9	142.2	28.0	33.4	35.9
PLA-3CsNP-s	0	61.9	110.1	170.8	35.8	38.2	42.3
	5.0	57.7	111.9	171.4	30.8	37.6	41.7
	10.0	55.6	109.5	170.2	32.5	36.9	40.9
	20.0	55.4	110.2	168.1	33.9	36.2	40.1
	25.0	53.7	115.1	168.7	37.5	37.2	41.2
	30.0	53.9	115.9	166.8	34.8	35.1	38.9
	35.0	53.4	114.4	170.4	32.8	34.0	37.7
	40	50.5	112.6	164.5	33.1	31.7	35.1

T_g (°C): glass transition, Tm (°C): melting temperature, T_c (°C): cold crystalline temperature, H_m (J/g): melting enthalpy, H_c (J/g): crystalline enthalpy, Xc (%): crystallinity

crystallization. Another factor that appears to increase the pace of crystallization due to radiation is a phenomenon known as nucleation. The huge crystallites or great orders are randomly destroyed by the radiation in this event, followed by the emergence of numerous and little crystallites [37]. With increasing irradiation dose, Tg and Tm for PLA-3CsNP irradiated in solution shift somewhat lower. In addition, there is a slight decrease in crystallinity. Furthermore, when the irradiation dose increases, the crystallization shifts to a higher temperature and broadens.

X-Ray Diffraction

The effect of gamma irradiation on polymer crystallinity was also investigated using X-ray diffraction patterns for

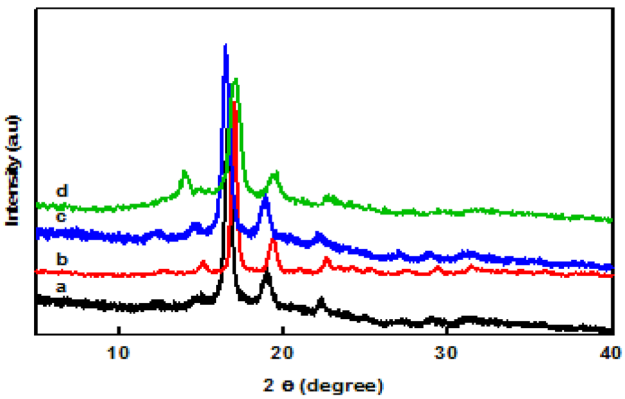

Fig. 9 XRD of **a** neat PLA, **b** γ-irradiated PLA in chloroform at 30 kGy, **c** PLA-3CsNP composite and **d** irradiated PLA-3CsNP composite at 30 kGy

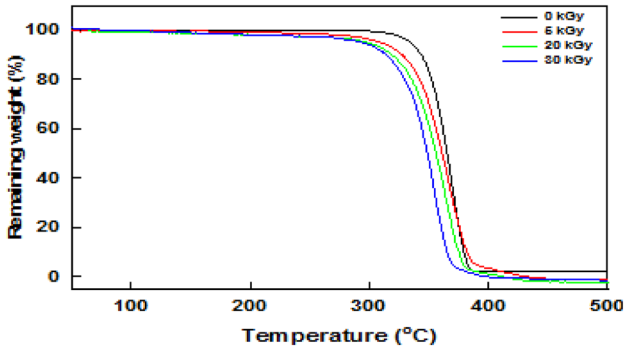

Fig. 10 TGA of unirradiated (0 KGy) and irradiated of PLA films at various γ-irradiation doses

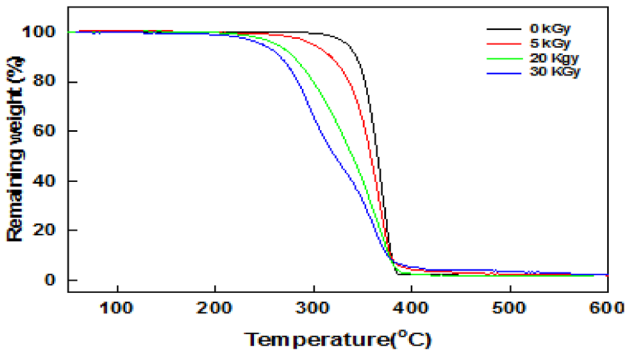

Fig. 11 TGA of unirradiated (0 KGy) and irradiated neat PLA in chloroform solution at various γ-irradiation doses

irradiated and non-irradiated samples. Results for unirradiated and irradiated neat PLA and PLA-3CsNP composite at 30 kGy are shown in Fig. 9. As can be seen, several diffraction peaks at 2θ = (14.7), (16.6), (18.9), and (22°) ascribed to α-form crystal in neat PLA and composite materials [38] are detected. With increasing total absorbed dose, the strength of the main diffraction peak occurs at (2θ = 16.6°) seems to grow, indicating somewhat enhancement in the degree of polymer crystallinity. This could be explained by the fact that gamma irradiation causes chain splitting mainly in amorphous regions, which is aided by oxidative reactions. As a result of the production of free radicals, crystallites form in the amorphous zone. Crosslinking of free radicals with other polymer chains appears to reduce crystallinity. These findings are consistent with previous research [39]. Irradiation causes these peaks to shift somewhat higher, implying that γ-irradiation causes some deformation of the PLA crystal structure. Thus, even for unirradiated or radiated test samples without and with CsNP filler, X-ray patterns reveal the presence of primarily α-form of crystalline structure of PLA.

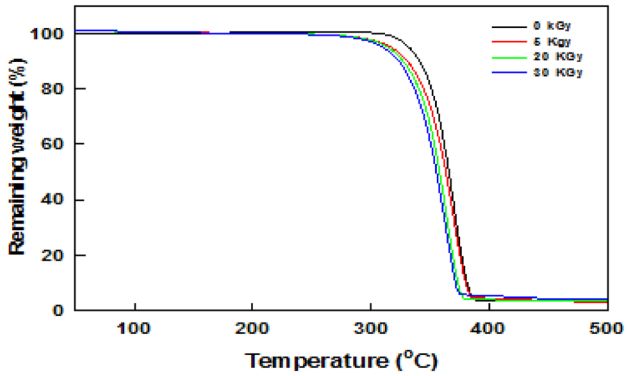

Fig. 12 TGA of unirradiated (0 KGy) and irradiated PLA-3CNP films at various γ-irradiation doses

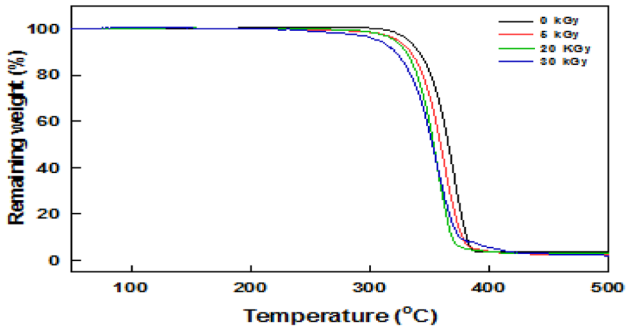

Fig. 13 TGA of unirradiated (0 KGy) and irradiated PLA-3CNP in chloroform solution at various γ-irradiation doses

Table 2 TGA data of PLA and PLA /3CNPs irradiated with γ-rays

Sample code	Dose (kGy)	$T_{0.5}$ (°C)	T_{max} (°C)
PLA-f	0	334	372
	5	309	366
	20	298	362
	30	294	355
PLA-s	5	300	365
	20	262	359
	30	248	363
PLA/3CsNP-f	0	331	372
	5	317	371
	20	313	370
	30	306	365
PLA/3CsNP-s	5	323	364
	20	319	359
	30	306	357

$T_{0.5}$ (°C): The temperature at which the half weight is lost

T_{max} (°C): The temperature at which the most weight is lost

Thermogravemetric Analysis

TGA was used to examine the effect of γ-irradiation on the thermal stability of neat PLA and PLA- 3CsNPcomposite, and the results are given in Figs. 10, 11, 12, 13. Table 2 lists thermal stability parameters such as the onset decomposition temperature ($T_{0.5}$), which is the temperature at 5% weight loss, and the maximal degradation temperatures (T_{max}). When comparing the TGA curves of unirradiated PLA and PLA-3CsNP composite, it is discovered that the addition of 3.0% CsNP reduces the $T_{0.5}$ (see Table 2) of the polymer matrix and results in one-stage weight loss in both samples. The thermal decomposition of polylactic acid produces cyclic oligomers, lactide, acetaldehyde, and carbon monoxide as end products. The maximal Tmax of pure PLA and PLA composite before irradiation are 372 and 372. As a result, adding 3% CsNP had no significant effect on thermal stability. The data show that after irradiation, both PLA and PLA composites have inferior thermal stability than unirradiated, as seen by the decrease in $T_{0.5}$ and Tmax values. The loss in thermal stability increases with increasing irradiation dose and is more noticeable for CH_3Cl solution irradiated samples than for irradiated films. The inclusion of PLA in chloroform hastens the thermal breakdown. A closer examination of the thermograms reveals that in the presence of CsNP, the decline in the thermal stability of PLA matrix caused by radiation treatment is minimized. The decrease in thermal stability could be linked to PLA matrix structure damage, which is more noticeable in samples irradiated in solution, as a result of the irradiation effect induced scission of carbonyl carbon–oxygen bonds and scission of carbonyl carbon–carbon linkages in the main chain, as well as bond cleavage of the CH_3 pendant groups to the main chain. PLA chains become more mobile and thus less thermally stable [35, 40].

Conclusions

PLA and PLA loaded with 3wt% CsNP in the solid state and in chloroform solution were exposed to gamma radiation (^{60}Co) at room temperature in the presence of oxygen. It was found that the γ-irradiation causes modifications in the structure of PLA matrix due to oxidative and partial crosslinking. The mechanical test revealed a considerable decrease in elongation and tensile strength at break, which increases with increasing irradiation dose, indicating that major chain scissions occurred at random. In comparison to samples irradiated in the solid state, the change is more pronounced in those irradiated in solution. The thermal characteristic results showed that whereas T_g and T_m for irradiated solid samples reduced little with increasing irradiation dose, both values dropped significantly for irradiated solution samples. Due to chain breakage caused by oxidative processes, crystallinity decreased as radiation exposure increased. The results also demonstrated that increasing the exposure irradiation dose lowered thermal stability, which was more noticeable for chloroform-irradiated samples compared to irradiated films. These results could be attributable to the irradiation induced chain scission of the PLA matrix. As a result, it was concluded that irradiation may have aided P LA and its composites biodegradation after use.

Acknowledgements The work's teams thank the Egyptian Petroleum Research Institute, National Center for Radiation Research and Technology, and Cairo University for their support

Author contribution GS, MF and AS were responsible for writing the manuscript. GS, ME and NM supervised the study. ME and GS were responsible for conducting the experiments and analyzing the data. All the authors read and approved the final manuscript.

Funding Open access funding provided by The Science, Technology & Innovation Funding Authority (STDF) in cooperation with The Egyptian Knowledge Bank (EKB).

Data Availability Data will be made available on request.

Declarations

Conflict of interest There is no conflict of interest and all authors have agreed with this submission and they are aware of the content.

References

1. Li L, Chen K, Zhang J (2022) Superelastic clay/silicone composite sponges and their applications for oil/water separation and solar interfacial evaporation. Langmuir 38:1853
2. Pekdemir S, Özen-Öner E, Pekdemir ME, Dalkılıç S, KadıoğluDalkılıç L (2022) An investigation into the influence of *C. moschata* leaves extract on physicochemical and biological properties of biodegradable PCL/PLA blend film. J Polym Environ 30:3645
3. Biswas MC, Jony B, Nandy PK, Chowdhury RA, Halder S, Kumar D, Ramakrishna S, Hassan M, Ahsan MA, Hoque ME, Imam MA (2021) Recent advancement of biopolymers and their potential biomedical applications. J Polym Environ 30:51–74
4. Erdem A, Dogan M (2020) Production and characterization of green flame retardant poly(lactic acid) composites. J Polym Environ 28:2837–2850

5. Scheid S-M, Juncheed K, Tanunchai B, Wahdan SFM, Buscot F, Noll M, Purahong W (2022) Interactions between high load of a bio-based and biodegradable plastic and nitrogen fertilizer affect plant biomass and health: a case study with *Fusarium solani* and mung bean (*Vigna radiata* L.). J Polym Environ 30:3534
6. Wu M, Chen Y, Peng P, Zuo D, Wang Q, Liu L, Liao S, Yi C (2022) Optimization of dark dyeing poly (lactic acid) yarn with indigo dyes applied to denim fabric. J Text Inst. https://doi.org/10.1080/00405000.2022.2047320
7. da Silva WA, Luna CBB, de Melo JBdCA, Araújo EM, Filho EAdS, Duarte RNC (2021) Feasibility of manufacturing disposable cups using PLA/PCL composites reinforced with wood powder. J Polym Environ 29:2932–2951
8. Radu E-R, Panaitescu DM, Nicolae C-A, Gabor RA, Rădiţoiu V, Stoian S, Alexandrescu E, Fierăscu R, Chiulan I (2021) The soil biodegradability of structured composites based on cellulose cardboard and blends of polylactic acid and polyhydroxybutyrate. J Polym Environ 29:2310–2320
9. Azizul Rahim FH, Saleh AA, Shuib RK, Ku Ishak KM, Abdul Hamid ZA, Abdullah MK, Shafiq MD, Rusli A (2021) Thermo-responsive shape memory properties based on polylactic acid and styrene-butadiene-styrene block copolymer. J Appl Polym Sci 138:51000
10. Little A, Wemyss AM, Haddleton DM, Tan B, Sun Z, Ji Y, Wan C (2021) Synthesis of poly (lactic acid-co-glycolic acid) copolymers with high glycolide ratio by ring-opening polymerisation. Polymers 13:2458
11. Rasal RM, Janorkar AV, Hirt DE (2010) Poly (lactic acid) modifications. Prog Polym Sci 35:338–356
12. Bednarek M, Borska K, Kubisa P (2020) Crosslinking of polylactide by high energy irradiation and photo-curing. Molecules 25:4919
13. Mangeon C, Renard E, Thevenieau F, Langlois V (2017) Networks based on biodegradable polyesters: an overview of the chemical ways of crosslinking. Mater Sci Eng, C 80:760–770
14. D'Anna A, Arrigo R, Frache A (2021) Rheology, morphology and thermal properties of a PLA/PHB/clay blend nanocomposite: the influence of process parameters. J Polym Environ 30:102–113
15. Liao C, Chen K, Li P, Li X, Zuo Y (2022) Nano-TiO_2 modified wheat straw/polylactic acid composites based on synergistic effect between interfacial bridging and heterogeneous nucleation. J Polym Environ 30:3021
16. Ávila Ramírez JA, Bovi J, Bernal C, Errea MI, Foresti ML (2020) Development of poly (lactic acid) nanocomposites reinforced with hydrophobized bacterial cellulose. J Polym Environ 28:61–73
17. Martinez Villadiego K, Arias Tapia MJ, Useche J, Escobar Macías D (2021) Thermoplastic starch (TPS)/polylactic acid (PLA) blending methodologies: a review. J Polym Environ 30:75–91
18. Mohamad SNK, Ramli I, Abdullah LC, Mohamed NH, Islam M, Ibrahim NA, Ishak NS (2021) Evaluation on structural properties and performances of graphene oxide incorporated into chitosan/poly-lactic acid composites: Cs/pla versus cs/pla-go. Polymers 13:1839
19. Kurakula M, Naveen NR (2021) Electrospraying: a facile technology unfolding the chitosan based drug delivery and biomedical applications. Eur Polymer J 147:110326
20. Seidi F, Yazdi MK, Jouyandeh M, Dominic M, Naeim H, Nezhad MN, Bagheri B, Habibzadeh S, Zarrintaj P, Saeb MR (2021) Chitosan-based blends for biomedical applications. Int J Biol Macromol 183:1818–1850
21. Elsawy MA, Saad GR, Sayed AM (2016) Mechanical, thermal, and dielectric properties of poly (lactic acid)/chitosan nanocomposites. Polym Eng Sci 56:987–994
22. Kongkaoroptham P, Piroonpan T, Pasanphan W (2021) Chitosan nanoparticles based on their derivatives as antioxidant and antibacterial additives for active bioplastic packaging. Carbohyd Polym 257:117610
23. Ito S, Miyazaki Y, Hirai N, Ohki Y (2021) Effects of gamma irradiation on the degradation of silicone rubber by steam exposure. J Nucl Sci Technol 58:166–172
24. Alsabbagh A, Abu Saleem R, Almasri R, Aljarrah S, Awad S (2020) Effects of gamma irradiation on 3D-printed polylactic acid (PLA) and high-density polyethylene (HDPE). Polym Bull 78:4931–4945
25. Kodal M, Wis AA, Ozkoc G (2018) The mechanical, thermal and morphological properties of γ-irradiated PLA/TAIC and PLA/OvPOSS. Radiat Phys Chem 153:214–225
26. Razavi SM, Dadbin S, Frounchi M (2014) Effect of gamma ray on poly(lactic acid)/poly(vinyl acetate-co-vinyl alcohol) blends as biodegradable food packaging films. Radiat Phys Chem 96:12–18
27. Shin BY, Han DH, Narayan R (2010) Rheological and thermal properties of the PLA modified by electron beam irradiation in the presence of functional monomer. J Polym Environ 18:558–566
28. Mihai M, Huneault MA, Favis BD, Li H (2007) Extrusion foaming of semi-crystalline PLA and PLA/thermoplastic starch blends. Macromol Biosci 7:907–920
29. Fekry M, Elmesallamy SM, El-Rahman NRA, Bekhit M, Elsaied HA (2022) Eco-friendly adsorbents based on abietic acid, boswellic acid, and chitosan/magnetite for removing waste oil from the surface of the water. Environ Sci Pollut Res Int 29:64633
30. Zou H, Yi C, Wang L, Liu H, Xu W (2009) Thermal degradation of poly(lactic acid) measured by thermogravimetry coupled to Fourier transform infrared spectroscopy. J Therm Anal Calorim 97:929–935
31. Chattopadhyay S, Chaki T, Bhowmick AK (2001) Structural characterization of electron-beam crosslinked thermoplastic elastomeric films from blends of polyethylene and ethylene-vinyl acetate copolymers. J Appl Polym Sci 81:1936–1950
32. Nugroho P, Mitomo H, Yoshii F, Kume T (2001) Degradation of poly (L-lactic acid) by γ-irradiation. Polym Degrad Stab 72:337–343
33. Vargas LF, Welt BA, Pullammanappallil P, Teixeira AA, Balaban MO, Beatty CL (2009) Effect of electron beam treatments on degradation kinetics of polylactic acid (PLA) plastic waste under backyard composting conditions. Packag Technol Sci 22:97–106
34. Haema K, Oyama TG, Kimura A, Taguchi M (2014) Radiation stability and modification of gelatin for biological and medical applications. Radiat Phys Chem 103:126–130
35. Yıldırım Y, Oral A (2018) Structural changes in Poly(lactic acid)–zeolite nanocomposites exposed to 60Co gamma rays. Radiat Eff Defects Solids 173:435–445
36. Milicevic D, Trifunovic S, Galovic S, Suljovrujic E (2007) Thermal and crystallization behaviour of gamma irradiated PLLA. Radiat Phys Chem 76:1376–1380
37. Luo S, Netravali A (1999) Effect of 60Co γ-radiation on the properties of poly (hydroxybutyrate-co-hydroxyvalerate). J Appl Polym Sci 73:1059–1067
38. Zhang J, Tashiro K, Tsuji H, Domb AJ (2008) Disorder-to-order phase transition and multiple melting behavior of poly (L-lactide) investigated by simultaneous measurements of WAXD and DSC. Macromolecules 41:1352–1357
39. Kolanthai E, Bose S, Bhagyashree K, Bhat S, Asokan K, Kanjilal D, Chatterjee K (2015) Graphene scavenges free radicals to synergistically enhance structural properties in a gamma-irradiated polyethylene composite through enhanced interfacial interactions. Phys Chem Chem Phys 17:22900–22910
40. Yıldırım Y, Oral A (2014) The influence of γ-ray irradiation on the thermal stability and molecular weight of Poly(l-Lactic acid) and its nanocomposites. Radiat Phys Chem 96:69–74